Connecting export fluxes to plankton food web efficiency in the Black Sea waters inflowing into the Mediterranean Sea

Constantin Frangoulis, Stella Psarra, Vasilis Zervakis, Travis B Meador, Paraskevi Mara, Alexandra Gogou, S Zervoudaki, Antonia Giannakourou, Vivi Pitta, Anna Lagaria, et al.

OXFORD UNIVERSITY PRESS Journal of Plankton Research

Connecting export fluxes to plankton food web efficiency in the Black Sea waters inflowing into the Mediterranean Sea

Journal:	*Journal of Plankton Research*
Manuscript ID:	JPR-2009-228.R1
Manuscript Type:	Original Article
Date Submitted by the Author:	22-Dec-2009
Complete List of Authors:	Frangoulis, Constantin; Hellenic Centre for Marine Research, Institute of Oceanography Psarra, Stella; Hellenic Centre for Marine Research, Inst. of Oceanography Zervakis, Vasilis; University of the Aegean, Dpt of Marine Science Meador, Travis; Woods Hole Oceanographic Institution, Dpt of Marine Chemistry and Geochemistry Mara, Paraskevi; University of Crete, Dpt of Chemistry Gogou, Alexandra; Hellenic Centre for Marine Research, Inst. of Oceanography Zervoudaki, S; Hellenic Centre for Marine Research, Inst. of Oceanography Giannakourou, Antonia; Hellenic Centre for Marine Research, Inst. of Oceanography Pitta, Vivi; Hellenic Centre for Marine Research, Inst. of Oceanography Lagaria, Anna; Hellenic Centre for Marine Research, Inst. of Oceanography Krasakopoulou, Eva; Hellenic Centre for Marine Research, Institute of Oceanography Siokou-Frangou, Ioanna; Hellenic Centre for Marine Research, Institute of Oceanography
Keywords:	plankton size spectra, downward flux, trophic transfer efficiency, Black Sea Water, Mediterranean

Connecting export fluxes to plankton food web efficiency in the Black Sea waters inflowing into the Mediterranean Sea

FRANGOULIS CONSTANTIN[1*], PSARRA STELLA[1], ZERVAKIS VASSILIS[2], MEADOR TRAVIS[3], MARA PARASKEVI[4], GOGOU ALEXANDRA[1], ZERVOUDAKI SOULTANA[1], GIANNAKOUROU ANTONIA[1], PITTA PARASKEVI[1], LAGARIA ANNA[1], KRASAKOPOULOU EVA[1], SIOKOU-FRANGOU IOANNA[1]

[1]HELLENIC CENTRE FOR MARINE RESEARCH, INSTITUTE OF OCEANOGRAPHY, GREECE
[2]UNIVERSITY OF THE AEGEAN, DEPARTMENT OF MARINE SCIENCES, GREECE
[3]WOODS HOLE OCEANOGRAPHIC INSTITUTION, DEPARTMENT OF MARINE CHEMISTRY AND GEOCHEMISTRY, WOODS HOLE, MA, USA
[4]UNIVERSITY OF CRETE, DEPARTMENT OF CHEMISTRY, CRETE

*CORRESPONDING AUTHOR: HELLENIC CENTRE FOR MARINE RESEARCH, INSTITUTE OF OCEANOGRAPHY, FORMER AMERICAN BASE OF GOURNES, PO BOX 2214, 71003, HERAKLION, CRETE GREECE, cfrangoulis@her.hcmr.gr

Keywords: plankton size spectra, downward flux, trophic transfer efficiency, Black Sea Water, Mediterranean

ABSTRACT

The short-time scale evolution of plankton carbon partitioning and downward flux in the modified Black Sea Water (BSW) mass entering the northeast Aegean Sea was studied using a Lagrangian approach (6-10/04/2008). The free-drifting sediment trap positioned at the bottom of the BSW layer and the control drifter, followed the same path within the anticyclone that circulates the BSW in the area. Zooplankton biomass increased (from 159 to 292 mg C m^{-2}), as did faecal pellet production (from 5 to 8 mg C m^{-2} day^{-1}), whereas a generally decreasing trend was displayed by POC (from 2099 to 1440 mg C m^{-2}), net primary production and biomass of plankton cells >5 μm (from 32 to 11 mg C m^{-2} day^{-1} and from 153 to 124 mg C m^{-2}, respectively). At the same time, the organic carbon flux increased (from 131 to 311 mg C m^{-2} day^{-1}), due to the contribution of zooplankton detritus (from 30 to 165 mg C m^{-2} day^{-1}). Normalized biomass-size spectra (NB-S) slopes suggest an elevated grazing pressure upon microplankton cells and a non-steady state ecosystem. Moreover,

both the overall shallow slope values and their high correlation to organic carbon flux indicate an increased efficiency of energy transfer to higher trophic levels.

INTRODUCTION

Plankton are a key component of the biological pump, incorporating carbon into their biomass in the surface ocean and subsequently, by their downward flux, to the ocean floor (De La Rocha and Passow, 2007). Identifying variability in plankton composition and its export out of the euphotic zone provides a basis for connecting plankton food web functioning and biogeochemical cycles. Downward flux is mainly channelled through the sinking of faecal pellets, marine snow and phytoplankton (Turner, 2002). The strong variability of the relative contribution of these three components to the downward flux and their remineralization rates depend on many factors including stocks, composition, size spectra, sinking velocities as well as plankton productivity and trophic interactions (Turner, 2002). The NB-S slopes of planktonic organisms have the potential to reveal the transfer efficiency of biomass (energy) to larger pelagic organisms and it has been suggested that these values can indicate the amount of carbon flux out of the upper ocean (San Martin *et al.*, 2006a).

The Aegean Sea is located in the Eastern Mediterranean Sea, which is characterised as one of the most oligotrophic seas of the world (Azov, 1986; Krom *et al.*, 2004). Oligotrophy is maintained despite the fact that the Aegean Sea receives an inflow of mesotrophic BSW mass in the northeast. This inflow consists of very light, brackish water, which is typically located in the uppermost layer (down to 20-30 m) of the Aegean Sea (Zervakis and Georgopoulos, 2002). The BSW mass is enriched in dissolved organic carbon (Sempéré *et al.*, 2002) and nitrogen rather than inorganic nutrients (Polat and Tugrul, 1996), and induces hydrological complexity (e.g. gyres and fronts) that can be highly mobile in time scales of the order of 10 days (Zervakis and Georgopoulos, 2002). These features result in plankton production that is among the highest of the Eastern Mediterranean for both autotrophs (Ignatiades *et al.*, 2002) and heterotrophs (Siokou-Frangou *et al.*, 2002), and the carbon flow within the pelagic food web seems to be quite efficient, affecting higher trophic levels (Stergiou *et al.*, 1997; Siokou-Frangou *et al.*, 2002). In addition, the front created in this area is characterized by increased plankton biomass and productivity (Isari *et al.*, 2006; Zervoudaki *et al.*, 2007), while the entire northeast Aegean Sea exhibits great spatial variability in hydrography and circulation, as well as in zooplankton communities on a scale of few km (Siokou-Frangou *et al.*, 2009).

Little is known regarding the downward flux of organic matter in the northeast Aegean except that this flux is more substantial than in the south Aegean (Lykousis *et al.*, 2002), which was assumed to be due to a more important export of the primary production (Siokou-Frangou *et al.*,

2002). Even less information exists on short-term variability (hours to days) of downward flux which has been proved to be as high as inter-seasonal flux variations, at a Western Mediterranean site (Goutx *et al.*, 2000). Thus, an emerging hypothesis for the area under the BSW influence is that short-term variability of downward flux can be significant.

The aim of the present study was to assess the short-time scale evolution of the organic carbon downward flux out of the BSW mass entering the Mediterranean Sea (northeast Aegean) in relation to water column plankton (stocks and rates) dynamics. Therefore, in order to follow a selected BSW mass, with minimum advection and mixing terms, a short-term Lagrangian study was carried out. Plankton stocks were examined in terms of composition, NB-S slopes and C and N stable isotopic signature. Overall, these data should provide information regarding the evolution of the ecosystem efficiency (as expressed by NB-S slopes) coupled to the geochemical fluxes along the BSW course into the northeast Aegean Sea.

METHOD

Experimental design

The strategy of the cruise (06-10 April 2008) was to use a multidisciplinary approach following the track of the BSW with Lagrangian drifters. The position of the BSW core was determined by satellite images of sea-surface temperature coupled with thermosalinograph records and CTD casts along the track of Lagrangian drifters (24.95-25.50^{o}E, 40.10-40.55^{o}N) (Fig. 1a, b). The latter consisted of a drifting sediment trap and a "control" drifter. The depth of the surface mixed layer (SML) occupied by the BSW was confined in the 0-16 m layer, as revealed by the CTD casts (Fig. 2) and therefore the sediment trap was deployed at 16 m depth. Drifters were designed following the TELEFOS drifter (Zervakis *et al.*, 2005) based on the standard Davis – CODE design (Davis, 1982) (George Messaritis Co., Greece). The second drifter (control, i.e. without trap) was deployed next to the drifting sediment trap in order to have an undisturbed control of the BSW track. Furthermore, comparison of their two tracks verified that the two instruments showed no windage, faithfully remaining in the same water body.

Several biogeochemical variables were studied in the sediment trap material and in the water column at 4 stations (3, 5, 6, 8); each station was sampled at the start of 4 successive trap deployment periods (A, B, C, D) that lasted from 0.3 to 1.3 days (Fig. 1c). Samples were additionally collected at station 2 prior to the first trap deployment at a nearby site. Water column samples were collected at 3, 10 and 20 m depth by means of a CTD-rosette. However, in order to compute the vertical fluxes out of the SML and given that the sediment trap was deployed at 16 m depth, the respective values of exported material at the bottom of the SML were obtained as the average of 10 and 20 m depth values. Mesozooplankton (200-2000 μm) samples were collected by

vertical tows of a WP2 200 µm mesh net (0-20 m layer). Special care was taken during sampling of sensitive organisms such as ciliates.

C and N elemental and isotopic analysis

For the determination of suspended POC and PON concentrations, 1.0-5.0 L of seawater, were filtered through pre-combusted (450 ºC), pre-weighed GF/F filters, then stored at -20 °C in the dark and analysed in the laboratory with a Thermo Scientific FLASH 2000 CHNS elemental analyser (Verardo *et al.*, 1990; Cutter and Radford-Knoery, 1991). Inorganic carbon was removed using 2 mol L^{-1} HCl.

For C and N stable isotopic analysis of sinking particulate organic matter (POM) 2-3 subsamples from sediment trap material were filtered through pre-combusted (450º C), pre-weighed GF/F filters and then stored at -20 °C until analysis. In the laboratory, GF/F filters were lyophilized until dry. For organic C and N elemental and isotopic analyses, filters were then sealed in a desiccator and exposed to an HCl vapour solution for >18 h. Samples were packaged into tin cups, and C and N content and stable isotopic composition were analyzed using a PDZ Europa elemental analyser interfaced with a isotope ratio mass spectrometer (Stable Isotope Facility, University of California Davis).

Picoplankton to mesozooplankton abundance in water column samples

For counts of heterotrophic bacteria and autotrophic cyanobacteria (*Synechococcus* spp. and *Prochlorococcus* spp., cell size 0.2-2 µm) 2ml duplicate water samples were fixed with paraformaldehyde (final concentration 1%), deep-frozen in liquid nitrogen and kept at –80 °C. Analysis was performed using a FACSCalibur (Becton Dickinson) flow cytometer equipped with a standard laser and filter set and using deionised water as sheath fluid. SYBRGreen I stain (Molecular Probe) was used to stain heterotrophic bacterial DNA.

For counts of auto- and heterotrophic nanoflagellates (AN and HN respectively, cell size: 1.5-20 µm), 30 mL water samples were fixed with borax-buffered formalin (final concentration 2%), stained with DAPI (Porter and Feig, 1980), and filtered onto black polycarbonate filters of 0.6 µm pore-size. AN and HN were distinguished using UV and blue excitation, then further classified in size categories and the biovolume was calculated.

Counting of larger nano- and micro- plankton (>5 µm cell size) was performed on samples preserved in alkaline (for diatoms, coccolithophorids and dinoflagellates) or acid (for ciliates) Lugol's solution (final concentration 2%) and refrigerated. Sub-samples of 100 mL were analysed after sedimentation for 24 h (Utermöhl, 1958). Cells were counted, distinguished into size-classes and major taxonomic groups and identified down to genus or species level. Cell sizes were

measured and converted into cell volumes using appropriate geometric formulae and image analysis (Image-pro plus 6.0).

Mesozooplankton samples were preserved in 4% buffered formaldehyde. Taxonomic identification was performed microscopically on subsamples (of known volume), further scanned for abundance and size determination by image analysis (Image-pro plus 6.0). Macrozooplankton (i.e. zooplankton >2000 µm) was also captured by the net, however since many empty size classes were present above 2000 µm, the latter was chosen as upper limit for the size spectra analysis.

Conversions of abundance data to carbon units

Heterotrophic bacterial abundance data were converted using 20 fg C $cell^{-1}$ (Lee and Fuhrman, 1987), 250 fg C $cell^{-1}$ for *Synechococcus* (Kana and Glibert, 1987) and 50 fg C $cell^{-1}$ for *Prochlorococcus* (Campbell *et al.*, 1994). The biovolume-carbon conversion factor was 183 fg C μm^{-3} for flagellates (Caron *et al.*, 1995) and 190 fg C μm^{-3} for ciliates (Putt and Stoecker, 1989). For larger phytoplankton, cell volumes per species were converted to carbon content applying appropriate conversion factors (Verity *et al.*, 1992; Montagnes *et al.*, 1994). The sizes of zooplankters were converted to carbon based on literature size-carbon relationships (Uye, 1982; Alcaraz *et al.*, 2003).

Primary production (PP)

Photosynthetic carbon fixation rates were estimated by means of the ^{14}C technique (Steemann Nielsen, 1952), as modified for the oligotrophic Eastern Mediterranean (Psarra *et al.*, 2000). Samples were placed in 250 mL polycarbonate bottles (3 light and 1 dark per depth), inoculated with 5 µCi of $NaH^{14}CO_3$ tracer, and incubated *in situ* for ca. 2h around midday, yielding maximum PP rates. Then samples were filtered onto 0.2 µm pore-size polycarbonate filters at <100 mm Hg vacuum pressure. Size fractionation onto 0.2, 2.0 and 5.0 µm polycarbonate filters (parallel filtration) allowed estimation of pico- (0.2-2.0), small nano- (2.0-5.0) and larger nano- and microphytoplankton (>5 µm) contributions. To remove excess ^{14}C-bicarbonate, filters were soaked in 1 mL 0.1 N HCl in uncapped polyethylene vials overnight and then counted using a Packard Liquid Scintillation Analyzer, after the addition of 4 mL of BSF scintillation cocktail. Daily (24h) net PP rates integrated in the 0-16 m layer were estimated (Moutin *et al.*, 1999).

Mesozooplankton faecal pellet production

For the measurement of mesozooplankton faecal pellet production, additional WP2 200 µm net vertical tows were performed in the upper 20 m. Animals were incubated in prefiltered (GF/F) seawater (four 250 mL bottles with a 100 µm mesh near the bottom) for 1 hour at the mean BSW

temperature. Then, animals were separated from pellets and preserved with 4% formalin. Pellets (number and size) were measured by inverted microscopy and mesozooplankton as described above (Image-pro plus 6.0). The largest mesozooplankton faecal pellet value (610 µm length and 1.43 x10^6 μm^3) was assumed to be the minimum size of macrozooplankton pellets and was used to distinguish meso- from macrozooplankton pellets in the trap. Faecal pellet volume was converted to carbon using Mediterranean literature values of faecal pellet density (Komar *et al.*, 1981), dry weight to wet weight ratio (Elder and Fowler, 1977) and carbon content per dry weight (Marty *et al.*, 1994).

Sediment-trap parameters

The sediment trap design was based on Knauer et al. (Knauer *et al.*, 1979) and consisted of a set of 8 PVC cylinders (8 x 65 cm) mounted on an aluminium cross frame and connected to one of the above-described drifters. All cylinders were previously filled with filtered seawater (0.2 µm) of increased salinity (plus ca. 3 psu), while a solution of ~4% buffered formalin was added as preservative in 3 of them. The other 5 cylinders were left unpreserved to avoid the "swimmer effect". Here we present analysis only from the unpreserved cylinders. The trap was deployed during 4 successive periods (varying from 0.3 to 1.3 days) (Fig. 1c). At the end of each deployment period the content of the unpreserved cylinders was gently mixed. Water sub-samples were taken in Lugol's alkaline solution and formalin for phytoplankton and ciliate microscopic analyses, respectively, and also filtered onto GF/F filters for elemental and stable C and N isotopic composition analyses (as described above). The remaining sample was examined for swimmers, which were removed (always <6% of the total zooplankters) and then concentrated (reverse filtration over a 20 µm mesh) and preserved with formalin for larger particle analysis. Low dilution subsamples were scanned, while high dilution subsamples were examined using an inverted microscope. Carcasses and faecal pellets sizes were converted to carbon as described above and corrected for carbon losses due to degradation (Lee and Fisher, 1994) considering the half-time of the trap deployment period.

Biomass-size spectra data processing

The above plankton biomass data from pico- to mesozooplankton (0.2 to 2000 µm) were integrated over the depth of the BSW water column and organised into NB-S, expressed in carbon units and plotted on a double logarithmic plot of normalised biomass versus particle size (Platt and Denman, 1978). Data were processed as in San Martin et al. (San Martin *et al.*, 2006a, b): the size classes with zero biomass and the inflection points at the interfaces between different methodologies were not included, as they can be subject to error resulting in curvature of the spectrum. Although the Platt and Denman model is sensitive to missing size ranges in the size spectrum, all depth-integrated complete

community spectra had an r^2 >0.98 and a significant regression slope (ANOVA, P <0.001) when anomaly data (see results) were disregarded. A one-way ANOVA was applied to investigate differences among NB-S slopes.

RESULTS

Hydrology, particle and plankton dynamics in the BSW layer

Both the control drifter and the drifting sediment trap followed an anticyclonic track (Fig. 1b) characterized by high speeds (40 ± 22 cm s^{-1}). Analysis of the salinity – temperature (T/S) characteristics of the water column along the drifter tracks revealed the presence of three distinct water types (Fig. 2). The surface layer was occupied by BSW having recently entered the Aegean Sea. Below the BSW mass, the water column was occupied by waters of Levantine Sea origin (S >38.5 psu). Between these two layers, and only at the northern part of the drifter track, was also a layer characterized by low salinity and temperature (Fig. 1b, Fig. 2). This layer is a remnant of BSW exiting the Dardanelles in winter (winter BSW), which remains in the North Aegean and gradually subsides under the lighter waters exiting the Dardanelles in spring (Zervakis and Georgopoulos, 2002).

The fully Lagrangian behaviour of both the sediment trap and the control drifter are confirmed not only by their identical tracks, but also by the fact that these tracks followed the core of the sea-surface salinity minimum, a clear index of "fresh" BSW in the region, as revealed by the ship's thermosalinograph (Fig. 1b). The evolution of the mean T/S characteristics of the surface water mass in the above-mentioned core is presented in Fig. 2, overlaid on a T/S diagram from all the CTD casts. As expected in a Lagrangian experiment, the T/S properties remain largely constant; the small changes that are observed are attributed to mixing with the underlying water masses of Levantine waters (mostly for stations 2, 3 and 8), and winter BSW (for stations 5 and 6). Hence, while the Lagrangian drifters followed the water parcels of the surface layer, the water characteristics in the subsurface layers changed due to the shear evident between the upper and lower layers.

Suspended POC decreased progressively along the drifter track from 2099 mg C m^{-2} to 1440 mg C m^{-2} (Fig. 3a). Similarly, the C:N ratio in suspended POM, with the exception of low values recorded at the first station, displayed a progressive decreasing trend from 9.3 to 7.7, though variability among stations was rather low (coefficient of variation 7.7%).

Phytoplankton carbon biomass (>5 μm) in the BSW was always dominated by dinoflagellates >10 μm, followed by small (5-10 μm) nanoflagellates (Fig. 3b), while coccolithophores and diatoms only represented <4 and <1% of total autotrophic biomass, respectively. A progressive decrease in all 4 phytoplankton groups' biomass was observed until station 5. After this station, diatom biomass

decreased further reaching minimum values (>4-fold decrease), whereas coccolithophores, nanoflagellates and small dinoflagellates increased again, leading to an overall increase of total phytoplankton biomass to slightly lower than the initial levels.

Meso- and macrozooplankton carbon biomass was always dominated by copepods, followed by chaetognaths and salps (Fig. 3c). A general tendency of biomass increase was observed for: (a) copepods >2 mm (*Calanus helgolandicus* adults and juveniles) and for mesozooplankton copepods (with the exception of station 6), and (b) for chaetognaths and total zooplankton biomass, after the first station. At station 2, only juvenile *C. helgolandicus* were collected (<2 mm). Big salps (maximum 5 cm) were seen at the sea surface all along the drifter track except at the last station; however WP2 net sampling collected them efficiently only at station 6, where their abundance was estimated to be greater than 1 specimen m^{-2}.

Primary productivity by larger nano- and microphytoplankton (>5 μm), representing cells mostly prone to sinking, was rather elevated at the first stations (32.53 mg C m^{-2} day^{-1}, at station 2), then displayed an almost 3-fold decrease from station 2 to station 6 (11.57 mg C m^{-2} day^{-1}), increased again at the last station a 2-fold increase thereafter (21.12 mg C m^{-2} day^{-1} at the last station) (Fig. 3d). These >5 μm phytoplankton cells, were responsible for 24 to 34% of total PP (Fig. 3d). Mesozooplankton faecal pellet production increased along the drifter track from 5.3 to 7.9 mg C m^{-2} day^{-1} (Fig. 3d).

Biogeochemistry and plankton dynamics of the exported material out of the BSW layer

The POC export out of the BSW layer ranged from 131 mg C m^{-2} day^{-1} at the first deployment period to 311 mg C m^{-2} day^{-1} at the last (Fig. 3e). The material identified was plankton cells, faecal pellets, zooplankton carcasses and marine snow. Plankton cells consisted of diatoms, coccolithophores, dinoflagellates and ciliates. Temporal dynamics of total phytoplankton C flux matched those of total POC flux, with plankton cells constituting always between 16 and 24% of the POC flux (Table I), and both displaying an overall 3-fold increase from period A to period D (Fig. 3f). Overall, phytoplankton community composition in the trap in terms of biomass was not significantly different from the overlying water column, with dinoflagellates again dominating, followed by coccolithophores and diatoms (Fig. 3f). Between the first and the last deployment periods, there was a 4-fold decrease in the percentage diatom contribution accompanied by a slight increase of coccolithophores and dinoflagellates, similar to the water column trends.

Faecal pellets were primarily cylindrical in shape (>99%), followed by few of rectangular shape. Zooplankton carcasses derived mostly from copepods, followed by chaetognaths and salps. Phytoplankton carbon flux exceeded both that of faecal pellets and zooplankton carcasses only in the first deployment period (Fig. 3f, g, h, Table I). Afterwards, faecal pellet and carcasses flux

increased, with carcasses becoming the dominant carbon flux over the last two deployment periods (~10-fold increase). Carcass flux was dominated by mesozooplankton, except during the last deployment period, where large copepod carcasses (*C. helgolandicus*) took over, with an overall >10-fold increase. Faecal pellets constituted the highest carbon flux during the second deployment period (Fig. 3h, Table I), and then decreased progressively, due to a decrease of macrozooplankton pellet flux. In contrast, the carbon flux of mesozooplankton faecal pellets increased progressively throughout the entire study (Fig. 3h).

A summary of export fluxes of organic carbon and nitrogen and the associated stable isotope compositions are reported in Table II. We observed a large range of carbon and nitrogen fluxes between sediment trap deployments, and also high variability between replicate samples of individual deployments. The coefficient of variation ranged from 15 to 44% for POC fluxes and from 5 to 19% for PON fluxes. The POC flux during deployment A was significantly lower than that of deployment B ($P<0.01$) while the final sediment trap deployment captured a significantly higher POC flux than all previous deployment periods ($P<0.01$). Deployment A also exhibited significantly lower PON export fluxes than deployments B and D ($P<0.04$). We observed no significant differences in the carbon to nitrogen ratios (C:N) between any of the deployments, however, an overall decreasing trend was observed (Fig. 3e).

The average stable carbon isotopic composition of exported POC ($\delta^{13}C$) was similar for each sediment trap deployment (approximately -24.0‰), and the variability between deployments was less than that observed between replicate traps of individual deployments (i.e. <1.0‰). The average of stable nitrogen isotopic composition ($\delta^{15}N$) of exported PON ranged from 4.8‰ to 0.4‰ and exhibited a decreasing trend over the course of the experiment. However, there was again considerable variability between replicate samples of individual deployments whereas $\delta^{15}N$ compositions were not significantly different between deployments. This variability could have resulted from the inclusion e.g. of a single, additional large copepod in a replicate sample.

Community normalised carbon biomass-size spectra

The NB-S slopes of the plankton community (pico- to mesozooplankton) in the BSW varied from -1.09 to -1.00, the shallowest slope being found at the last station (Fig. 4a, b). These slopes were not significantly different between stations ($P>0.1$). Interestingly, a trough anomaly in the slopes of these size spectra was present (Fig. 4a) at the size classes corresponding to large plankton cells (>50 µm ESD) which were dominated by ciliates. This anomaly was more or less present at all stations except station 3 (Fig. 4a), where the lowest meso- and macrozooplankton biomass was observed (Fig. 3c). After disregarding these anomalies, r^2 in all stations increased above 0.98 and slope values were slightly changed (<1%).

The temporal evolution of the BSW NB-S slopes (Fig. 4b) was not significantly correlated to that of the water column parameters (Fig. 3a, b, c, d) except with the biomass of total zooplankton (excluding salps) and that of copepods (both r^2>0.94, P<0.01). The NB-S slopes obtained at the station corresponding to the beginning of each trap deployment period were plotted against estimates of total exported POC (i.e. the sum of cells, carcasses and faecal pellets carbon) captured during that period and found to be highly correlated (r^2 = 0.93, P<0.01) (Fig. 4c).

DISCUSSION

The BSW entering the Aegean Sea is known to create a thin surface layer of brackish water, overlying the highly saline waters of Levantine origin (Zervakis and Georgopoulos, 2002). In the present study this water mass was observed in the upper 16 m of the water column. In addition, the hydrology in the region is characterised by the presence of a fast permanent anticyclone around the island of Samothraki which circulates the surface BSW layer within the North Aegean (Zervakis and Georgopoulos, 2002). The anticyclonic circulation increases the residence time of the BSW mass by "trapping" it in the interior of the anticyclone. Both drifters deployed followed the same path along the periphery of this permanent anticyclone and the CTD profiles obtained along this track indicated a progressive salinity modification of the BSW, however, this modification through vertical mixing was delayed by the presence, at the northern edges of the anticyclone, of a layer characterized by low salinity and temperature, which is a remnant of a winter BSW layer (Zervakis and Georgopoulos, 2002) (Fig. 2).

Biogeochemistry, food-web and export dynamics of the BSW layer

Most of the biochemical parameters displayed strong temporal variability with rather progressive trends. Similar overall increasing trends were only observed for zooplankton biomass and mesozooplankton faecal pellet production with their respective downward fluxes. Due to the shallow, short-time sediment trap deployments (i.e. reduced degradation) and the high sinking velocities of zooplankton carcasses and faecal pellets (>25 m day^{-1}) (Frangoulis *et al.*, 2005), most of the latter were quickly exported to the bottom of the BSW. Moreover, the C:N ratios both in suspended and exported POM displayed an overall decreasing trend. Minimum C:N ratios recorded at the end of the experiment denote a relatively "fresher" material (Gordon and Cranford, 1985), indicative of enhanced *in situ* production and increased plankton metabolic and growth rates. This is confirmed by the simultaneous increase of zooplankton biomass, faecal pellet production and zooplankton detritus flux. On the other hand, opposite POC trends were observed, with suspended POC values decreasing gradually along the drifter track (except for a slight increase at the last station), whereas the respective POC flux in the trap significantly increased.

Suspended POC concentration (79-131 mg C m^{-3}) was higher than that reported (8-56 mg C m^{-3}) for different regions in the E. Mediterranean (Ediger *et al.*, 2005; Seritti *et al.,* 2003), but was within the range (20-196 mg C m^{-3}) of that measured in the N. Aegean during Spring (Krasakopoulou *et al.*, 2002). Previous studies suggest that these high POC values may originate from river runoff or local biogenic production rather than from the BSW inflow (Karageorgis *et al.*, 2003).

POC flux values in this study were higher than those recorded down to 50 m for the rest of the Aegean Sea and other open Mediterranean waters (e.g. Moutin and Raimbault, 2002). This high export may be attributed to the elevated primary production in the northeast Aegean, especially during Spring, through an efficient omnivorous planktonic food web in this area (Siokou-Frangou *et al.*, 2002; Zervoudaki *et al.*, 2007). It has been well documented that sedimentation in the form of fresh phytoplankton material is highest during periods of new production in shelf seas (Smetacek, 1984). However, although the total net primary production values measured here for the 0-16 m layer were elevated (74.6 ± 32.6 mg C m^{-2} day^{-1}, deriving from Figure 3d), typical for spring values in the area (41.5-157.1 mg C m^{-2} h^{-1}, for the 0-100 m layer) (Ignatiades *et al.*, 2002), they are insufficient to explain the high values of POC flux, which far exceed those of primary production by cells >5 μm. Neither can these primary production values be attributed to mineral nutrient concentrations that were very low and displayed a decreasing trend in the BSW layer during this study (NO_3+NO_2: 0.11 ± 0.07 μmol L^{-1}, PO_4: 4.4 ± 0.5 nmol L^{-1}, unpublished data), unless these low nutrient concentrations are due to uptake processes. Moreover, the percentage contribution of daily primary production (>5 μm) (Fig. 3d) to the respective phytoplankton C flux (Fig. 3f) displayed a sharp decrease from 93.5% at the first deployment to 28.4%, at the last deployment. This might be attributed to the progressive decrease in primary production, which in turn could be related to the progressive exhaustion of DIN. A most probable explanation, however, could be that phytoplankton cells becoming less active after mineral nutrient exhaustion tend to sediment at higher rates, thus contributing to the increase of POC flux. It is worth noting however, that a direct comparison of phytoplankton biomass and/or daily primary production to the respective phytoplankton C flux would be misleading due to low sinking velocities of phytoplankton natural assemblages compared to larger organisms and particles, namely zooplankton cells and carcasses, as described above. Whole phytoplankton community sinking velocities in experimental mesocosms during a spring diatom bloom ranged from 0.29 to 1.53 m day^{-1} (Riebesell, 1989). In this study, with mixed natural nano- and microphytoplankton assemblages dominated by smaller cells (namely dinoflagellates), lower sinking velocities would be anticipated. Therefore, even if maximum sinking rates of 1.53 m day^{-1} were be applied in our data, and depending on the vertical distribution of phytoplankton cells, a minimum of 5 to 10 days would be required for them to sink

to the bottom of the BSW. Given the time scale of the present study this point leads to a decoupling of primary production and suspended phytoplankton biomass from the respective phytoplankton C flux. Apparently, temporal dynamics of the latter reflect the state of the BSW phytoplankton dynamics, at a time period some days prior to the beginning of our experiment.

Overall, phytoplankton C flux constituted a rather consistent component of the total POC flux (16 to 24%), whereas zooplankton detritus (faecal pellets and carcasses) constituted a higher but more variable contribution, always exceeding 60% of the POC flux, after the first deployment period.

The faecal pellet C flux and its contribution to the total POC flux in this study (10 to 53%) was higher than that reported in the oligotrophic South Aegean (<6% at 200 m depth) (Wassmann *et al.*, 2000) and in the open Western Mediterranean (6 to 30% at 50 m, Fowler *et al.*, 1991). This faecal flux was initially dominated by macrozooplankton faecal pellets and at the end by mesozooplankton faecal pellets. Considering the dominance of cylindrical pellets in the trap and that of copepods in the water column, the origin of mesozooplankton faecal pellet flux appears to be copepods. However, the origin of the cylindrical macrozooplankton faecal pellets is less evident. Salp faecal pellets are excluded, as they are known to produce rectangular pellets (Frangoulis *et al*., 2005). Although large copepods (*C. helgolandicus*) could explain a fraction of the large pellets, the size of some cylindrical pellets exceeded the size of *C. helgolandicus* body. The larger cylindrical pellets could originate from chaetognaths (Dilling and Alldredge, 1993) which were found in the water column, and/or other larger crustacean (e.g. euphausiids). The latter were not captured with the WP2 net but may have been present in the water column and/or migrated into the BSW only during the night.

Sinking zooplankton carcasses also constituted an important C flux, exhibiting a progressive increase over the course of the experiment, becoming the dominant organic carbon flux (>40%) in the last two trap deployment periods. This increase could be related to the progressive increase in zooplankton biomass observed in the water column and/or to a parallel progressive increase of non-predatory mortality rate. The latter may be due to the progressive exhaustion of larger phytoplankton (namely diatoms), resulting in the higher zooplankton detritus export recorded at the last deployment period. Comparison of carcass flux with other studies is difficult as there are few studies that accurately measure this flux. To our knowledge, no such measurements exist in the open Mediterranean, and the only flux estimates (at 200 m) derived from a model study applied in the NW Mediterranean, which estimated a maximum carcass C flux of 6.3 mg C m^{-2} day^{-1} (Andersen and Nival, 1988). This flux was lower than our minimum values (14.3 mg C m^{-2} day^{-1}).

The above elevated C flux originating from zooplankton faecal pellets and carcasses, together with the observed trends in the water column zooplankton, suggest that the latter were favoured by the environment. These trends involve an overall increase of the mesozooplankton, chaetognaths

and macrozooplankton copepod biomass, as well as that of mesozooplankton faecal pellet production. As the latter probably results from increased food consumption, this might partially account for the observed decrease in primary production and the biomass of larger phytoplankton cells during the first half of the study, thus resulting in a respective increase of heterotrophic to autotrophic biomass ratio (for organisms >5 μm ESD: from 4.2 at the first station to 9.5 at the last one). The increase of this ratio coupled to the increase of zooplankton biomass and faecal pellet production, could suggest that zooplankton inhabiting the BSW layer enhanced their production (biomass) and grazing along the anticyclonic track of the incoming water mass.

As stated above, we observed increasing trends of POC and PON fluxes, and a decreasing, though not significant, trend in C:N composition of sinking particles over the course of the experiment. The above trends coincided with an increasing trend in phytoplankton sinking flux (3-fold), but mostly with that in zooplankton carcasses (~10-fold) and its relative contribution to the total POC export (Fig. 3). Significant shifts in the stable isotopic composition of sinking POC or PON were not observed during the sediment trap deployment period. The $\delta^{13}C$ signatures of all sediment trap deployments were similar throughout the experiment (-24.0‰ to -24.5‰). These values are slightly lighter than typical marine values (ca. -21‰) (e.g. Michener and Shell, 1994) and may be indicative of terrigenous inputs to the system. The $\delta^{15}N$ signatures showed a general decreasing trend during the sampling period (from 4.6 ± 2.8‰ to 0.4 ± 3.4‰, Table II) but were highly variable both between deployments and between replicate samples of the sediment traps. Given the substantial variability between replicates, it is difficult to interpret the $\delta^{15}N$ data. The changes in the relative contribution of phytoplankton, zooplankton, and faecal pellets to the sinking flux (Table I) captured by individual traps of each deployment appear to have dramatically altered the integrated $\delta^{15}N$ signal. We note, however, that the significant increases of sinking zooplankton carcasses during the sampling period did not coincide with similar increases in the $\delta^{15}N$ signature of the sinking PON flux, as predicted by the ~3‰ isotopic enrichment of ^{15}N that is expected as N is transferred to higher trophic levels (Checkley and Miller, 1989). Suspended PON and mesozooplankton collected from the water column at 3 stations during this study also exhibited decreasing trends in $\delta^{15}N$ signatures, ranging from 4.0 ± 1.8‰ to 1.3 ± 0.1‰, and from 5.4 ± 0.3‰ to 4.1 ± 1.2‰, respectively (unpublished data). The spatiotemporal trends in both suspended and sinking PON of the evolving water mass suggest a shift in the $\delta^{15}N$ composition of N that was initially assimilated into the food webs of these regions. This shift, from an isotopically enriched to depleted N source, coincided with increased fluxes of POC, PON, and zooplankton carcases. This could have resulted from the removal (i.e. sinking) of ^{15}N-enriched PON and an increased contribution of ^{15}N-depleted recycled N to production during the evolution of the BSW mass.

Characteristics of community normalised carbon biomass-size spectra

The overall shallow NB-S slopes (-1.09 to -1.00) indicate that there is more biomass transferred to higher trophic levels than might have been expected at equilibrium. This confirms a previous suggestion that the northeast Aegean ecosystem has a higher efficiency of carbon (energy) transfer channelled to mesozooplankton compared to the rest of the Aegean Sea (Siokou-Frangou *et al.*, 2002).

Interestingly, NB-S slopes in this study confirm their potential to reveal the efficiency of carbon flux not only to higher trophic levels but also as sinking out of the upper mixed layer (Richardson *et al.*, 2004). This is shown by the strong relationship between NB-S slopes and the total estimated organic carbon flux (Fig. 4c): higher trophic transfer efficiency indicated by shallower slopes corresponded to higher downward carbon export (end phase), relative to a lower trophic transfer efficiency indicated by steeper slopes, coinciding with a lower downward carbon export out of the BSW (initial phase). In addition, the higher C export values (shallower slopes) corresponded to a higher percentage contribution from higher trophic levels (i.e. zooplankton faecal pellets and carcasses) than under lower C flux values (steeper slopes). The observed relationship between NB-S slopes and carbon fluxes could be due to the fact that both constitute integration over recent time. In contrast, the lack of relationship between the NB-S slopes and the stock/production data (e.g. biomass, primary production), as found in the present study (except for zooplankton biomass) and in San Martin et al. (San Martin *et al.*, 2006b), could be attributed to the fact that the latter represent instantaneous measures.

Another peculiarity of the NB-S slopes determined in this study was the anomaly encountered in the size spectra (Fig. 4a). Such an anomaly (i.e. the shift towards lower biomass values) may correspond to excess mortality or migration losses (Zhou, 2006) at that particular section of the spectrum. This anomaly appeared in the carbon size classes that correspond to larger phytoplankton and ciliates biomass. Given the low migration capacity of these organisms, the most probable explanation for this anomaly is high mortality, namely due to grazing pressure. This phenomenon appears to be enhanced in the northeast Aegean, where a strong grazing impact by copepods on ciliates was recorded together with an important consumption of primary production (Zervoudaki *et al.*, 2007), supporting a previous hypothesis of strong top-down control of the ciliate population in this area (Pitta and Giannakourou, 2000). The absence of this anomaly at station 3 (Fig. 4a), where the lowest meso- and macrozooplankton biomass was encountered (Fig. 3c), further enhances this hypothesis.

The theoretical value predicted by a model characterising a near-steady state open ocean pelagic system, in terms of carbon, is -1.22 (Platt and Denman, 1978). The NB-S slopes of the present study (-1.09 to -1.00) being shallower than the above theoretical value imply a non-steady state

ecosystem. However, it is important to emphasize that it is more the regularity and the linearity of the NB-S spectrum, and not the numerical value of the slope alone that may characterise a close-to steady state system (Quinones *et al.*, 2003). Therefore, the above mentioned anomaly recorded in the NB-S further supports a non-steady state condition of the ecosystem.

CONCLUSIONS

During this experiment, the substantial variability observed for most biogeochemical variables confirms our original hypothesis that the area under the BSW influence exhibits significant variability in downward flux on short-time scales. The strongest signal was the increase of carbon export out of the BSW, essentially due to a sharp increase of the contribution of zooplankton detritus. A parallel increase in zooplankton biomass and faecal pellet production in the overlying BSW layer, in combination with the overall shallow NB-S slopes, confirmed the hypothesis of a more efficient energy transfer to higher trophic levels in the northeast Aegean Sea, as suggested by previous studies. The recorded anomaly in the NB-S slopes hints at an elevated grazing pressure upon ciliates and larger phytoplankton and a non-steady state condition of the ecosystem. Overall, this study provided evidence for connecting BSW plankton food web efficiency (as expressed by NB-S slopes) to carbon export fluxes in a Mediterranean area affected by the BSW inflow.

ACKNOWLEDGEMENTS

We are grateful to A.C. Banks for providing satellite images and to K. Tsiaras for model predictions of current fields. We thank T. Zoulias, T. Moutsopoulos for support in the field and the captain and the crew of R/V 'Aegaeo' for shipboard assistance. Thanks also to S. Stavrakakis, K. Christodoulou and M. Pettas for help in the design and construction of the sediment traps as well as to I. Magiopoulos for flow cytometry analysis and K. Charalambous for CHN analysis. We also thank three anonymous reviewers and the Associate Editor for helpful comments on the manuscript. Research for this paper was supported by the SESAME project (contract no. 036949), supported by the European Commission's Sixth Framework Programme on Sustainable Development, Global Change and Ecosystem.

REFERENCES

Alcaraz, M., Saiz, E., Calbet, A. *et al.* (2003) Estimating zooplankton biomass through image analysis. *Mar. Biol.*, **143**, 307-315.

Andersen, V. and Nival, P. (1988) A pelagic ecosystem model simulating production and sedimentation of biogenic particles : role of salps and copepods. *Mar. Ecol. Prog. Ser.*, **44**, 37-50.

Azov, Y. (1986) Seasonal patterns of phytoplankton productivity and abundance in nearshore oligotrophic waters of the Levant Basin (Mediterranean). *J. Plankton Res.*, **8**, 41-53.

Campbell, L., Nolla, H. A. and Vaulot, D. (1994) The importance of *Prochlorococcus* to community structure in the Central of Pacific Ocean. *Limnol. Oceanogr.*, **39**, 954-961.

Caron, D. A., Dam, H. G., Kremer, P. *et al.* (1995) The contribution of microorganisms to particulate carbon and nitrogen in surface waters of the Sargasso Sea near Bermuda. *Deep-Sea Res.*, **42**, 943-972.

Checkley, D. M. and Miller, C. A. (1989) Nitrogen isotope fractionation by oceanic zooplankton. *Deep-Sea Res.*, **10**, 1449-1456.

Cutter, G. A. and Radford-Knoery, J. (1991) Determination of carbon, nitrogen, sulfur and inorganic sulfur species in marine particles. In Hurd, D. C. and Spencer, D. W. (eds), *Marine Particles: Analysis and Characterization, Geophysical Monograph 63,* pp. 57-63.

Davis, R. E. (1982) An inexpensive drifter for surface currents. *Proceedings of the IEEE Second Working Conf. on Current Measurement Hilton Head, U.S.A.*, pp. 89-93.

De La Rocha, C. and Passow, U. (2007) Factors influencing the sinking of POC and the efficiency of the biological carbon pump. *Deep-Sea Res.*, **54**, 639-658.

Dilling, L. and Alldredge, A. L. (1993) Can chaetognath fecal pellets contribute significantly to carbon flux? *Mar. Ecol. Prog. Ser.*, **92**, 51-58.

Ediger, D., Tugrul, S. and Yilmaz, A. (2005) Vertical profiles of particulate organic matter and its relationship with chlorophyll-a in the upper layer of the NE Mediterranean Sea. *J. Mar. Syst.*, **55**, 311-326.

Elder, D. L. and Fowler, S. W. (1977) Polychlorinated Biphenyls: Penetration into the deep ocean by zooplankton fecal pellet transport. *Science*, **197**, 459-461.

Fowler, S. W., Small, L. F. and La Rosa, J. (1991) Seasonal particulate carbon flux in the coastal Northwestern Mediterranean Sea, and the role of zooplankton fecal matter. *Oceanol. Acta*, **14**, 77-85.

Frangoulis, C., Christou, E. D. and Hecq, J. H. (2005) Comparison of marine copepod outfluxes: nature, rate, fate and role in the carbon, and nitrogen cycles. *Adv. Mar. Biol.*, **47**, 251-307.

Gordon, C. D. and Cranford, J. P. (1985) Detailed distribution of dissolved and particulate organic matter in the Arctic Ocean and comparison with other oceanic regions. *Deep-Sea Res.*, **32**, 1221-1232.

Goutx, M., Momzikoff, A., Striby, L. *et al.* (2000) High-frequency fluxes of labile compounds in the central Ligurian Sea, Northwestern Mediterranean. *Deep-Sea Res.*, **47**, 533-556.

Ignatiades, L., Psarra, S., Zervakis, V. *et al.* (2002) Phytoplankton size-based dynamics in the Aegean Sea (Eastern Mediterranean). *J. Mar. Syst.*, **36**, 11-28.

Isari, S., Ramfos, A., Somarakis, S. *et al*. (2006) Mesozooplankton distribution in relation to hydrology of the Northeastern Aegean Sea, Eastern Mediterranean. *J. Plankton Res.*, **28**, 241-255.

Kana, T. and Glibert, P. M. (1987) Effect of irradiances up to 2000 μE m^{-2} s^{-1} on marine *Synechococcus* WH 7803-I. Growth, pigmentation and cell composition. *Deep-Sea Res.*, **34**, 479-516.

Karageorgis, A. P., Kaberi, H. G., Tengberg, A. *et al*. (2003) Comparison of the particulate matter distribution between a mesotrophic and an oligotrophic marine area: the Skagerrak Sea and the northeastern Aegean Sea. *Cont. Shelf Res.*, **23**, 1787-1809.

Knauer, G. A., Martin, J. H. and Bruland, K. W. (1979) Fluxes of particulate carbon, nitrogen, and phosphorus in the upper water column of the northeast Pacific. *Deep-Sea Res.*, **26**, 97-108.

Komar, P. D., Morse, A. P., Small, L. F. *et al*. (1981) An analysis of sinking rates of natural copepod and euphausiid fecal pellets. *Limnol. Oceanogr.*, **26**, 172-180.

Krasakopoulou, E., Zeri, C. and Kaberi, H. (2002) Spatial and temporal variability of organic matter in the NE Aegean Sea. International Conference, Oceanography of the Eastern Mediterranean and Black Sea: Similarities and differences of two interconnected basins, 14-18 October 2002, Ankara, Turkey, pp 295.

Krom, M., Herut, B. and Mantoura, R. F. C. (2004) Nutrient budget for the Eastern Mediterranean: Implications for phosphorus limitation. *Limnol. Oceanogr.*, **49**, 1582-1592.

Lee, S. and Furhrman, J. A. (1987) Relationships between biovolume and biomass of naturally derived marine bacterioplankton. *Appl. Envir. Microbiol*., **53**, 1298-1303.

Lee, B. G. and Fisher, N. S. (1994) Effects of sinking and zooplankton grazing on the release of elements from planktonic debris. *Mar. Ecol. Prog. Ser.*, **110**, 299-307.

Lykousis, V., Chronis, G., Tselepides, A. *et al*. (2002) Major outputs of the recent multidisciplinary biogeochemical researches undertaken in the Aegean Sea. *J. Mar. Syst.*, **33-34**, 313-334.

Marty, J. C., Nicolas, E., Miquel, J. C. *et al*. (1994) Particulate fluxes of organic compounds and their relationship to zooplankton faecal pellets in NW Mediterranean sea. *Mar. Chem.*, **46**, 387-405.

Michener, R. H. and Shell, D. M. (1994) Stable isotope ratios as tracers in marine and aquatic food webs. In Lajtha, K. and Michener, R. H. (eds), *Stable isotopes in ecology and environmental science.* Blackwell Scientific Publications, Oxford, pp. 138-157.

Montagnes, S. J. D., Berges, A. J., Harrison, J. P. *et al*. (1994) Estimating carbon, nitrogen, protein, and chlorophyll a from volume in marine phytoplankton. *Limnol. Oceanogr.*, **39**, 1044-1060.

Moutin, T. and Raimbault, P. (2002) Primary production, carbon export and nutrients availability in western and eastern Mediterranean Sea in early summer 1996 (MINOS cruise). *J. Mar. Syst*., **33-34**, 273-288.

Moutin, T., Raimbault, P. and Poggiale, J. C. (1999) Production primaire dans les eaux de surface de la Mediterranee occidentale. Calcul de la production journaliere. *C. R. Acad. Sci.*, **322**, 651-659.

Pitta, P. and Giannakourou, A. (2000) Planktonic ciliates in the oligotrophic Eastern Mediterranean: Vertical, spatial distribution and mixotrophy. *Mar. Ecol. Prog. Ser.*, **194**, 269-282.

Platt, T. and Denman, K. (1978) The structure of pelagic ecosystems. *Rapp. P. -v., Reun. Cons. int. Explor. Mer*, **173**, 60-65.

Polat, C. and Tugrul, S. (1996) Chemical exchange between the Mediterranean and the Black Sea via the Turkish straits. Dynamics of Mediterranean Straits and Channels. CIESM Science Series no.2. *Bull. Inst. Oceanogr. Monaco*, special **17**, 167-186.

Porter, K. G. and Feig, Y. S. (1980) The use of DAPI for identifying and counting aquatic microflora. *Limnol. Oceanogr.*, **25**, 943-948.

Psarra, S., Tselepides, A. and Ignatiades, L. (2000) Primary productivity in the oligotrophic Cretan Sea (NE Mediterranean): seasonal and interannual variability. *Prog. Oceanogr.*, **46**, 187-204.

Putt, M. and Stoecker, D. K. (1989) An experimentally determined carbon volume ratio for marine oligotrichous ciliates from estuarine and coastal waters. *Limnol. Oceanogr.*, **34**, 1097-1103.

Quinones, R. A., Platt, T. and Rodriguez, J. (2003) Patterns of biomass-size spectra from oligotrophic waters of the Northwest Atlantic. *Prog. Oceanogr.*, **57**, 405-427.

Richardson, T. L., Jackson, G. A., Ducklow, H. W. *et al*. (2004) Carbon fluxes through food webs of the eastern equatorial Pacific: an inverse approach. *Deep-Sea Res.*, **51**, 1245-1274.

Riebesell, U. (1989) Comparison of sinking and sedimentation rate measurements in a diatom winter/spring bloom. *Mar. Ecol. Prog. Ser.*, **54**, 109-119.

San Martin, E., Harris, R. P. and Irigoien, X. (2006a) Latitudinal variation in plankton size spectra in the Atlantic Ocean. *Deep-Sea Res.*, **53**, 1560-1572.

San Martin, E., Irigoien, X., Harris, R. P. *et al*. (2006b) Variation in the transfer of energy in marine plankton along a productivity gradient in the Atlantic Ocean. *Limnol. Oceanogr*. **51**, 2084–2091.

Sempéré, R., Panagiotopoulos, C., Lafont, R. *et al*. (2002) Total organic carbon dynamics in the Aegean Sea. *J. Mar. Syst.*, **33-34**, 355-364.

Siokou-Frangou, I., Bianchi, A., Christaki, U. *et al*. (2002) Organic carbon partitioning and carbon flow in the planktonic food web along a gradient of oligotrophy in the Aegean Sea (Mediterranean Sea). *J. Mar. Syst.*, **33-34**, 335-353.

Seritti, A., Manca, B.B., Santinelli, C. *et al*. (2003) Relationships between dissolved organic carbon (DOC) and water mass structures in the Ionian Sea (winter 1999). *J. Geophys. Res*. **108**. doi:10.1029/2002JC001345.

Siokou-Frangou, I., Zervoudaki, S., Christou, E. *et al*. (2009) Variability of mesozooplankton spatial distribution in the North Aegean Sea as influenced by the Black Sea waters outlfow. *J. Mar. Syst.*, 78, 557–575.

Smetacek, V. (1984) The supply of food to the benthos. In Fasham, M. J. R. (ed.), *Flows of energy and materials in marine ecosystems. Theory and practice.* Plenum Press, New York, pp. 517-546.

Steemann Nielsen, E. (1952) The use of radioactive carbon (14C) for measuring organic production in the sea. *J. Cons. Int. Explor. Mer*, **18**, 117-140.

Stergiou, K. I., Christou, E. D., Georgopoulos, *et al.* (1997). The Hellenic seas: physics, chemistry, biology and fisheries. *Ocean. Mar. Biol. Annu. Rev*. **35**, 415– 538.

Turner, J. T. (2002) Zooplankton fecal pellets, marine snow and sinking phytoplankton blooms. *Aquat. Microb. Ecol.*, **27**, 57-102.

Utermöhl, H. (1958) Zur vervollkommnung der quantitativen Phytoplankton Methodik. *Mitt. Int. Ver. Theor. Angew. Limnol.*, **9**, 1-38.

Uye, S. (1982) Length-weight relationships of important zooplankton from the Inland Sea of Japan. *J. Oceanogr. Soc. Japan*, **38**, 149-158.

Verardo, D. J., Froelich, P. N. and McIntyre, A. (1990) Determination of organic carbon and nitrogen in marine sediments using the Carlo Erba NA-1500 Analyzer. *Deep-Sea Res.*, **37**, 157-165.

Verity, P. G., Robertson, C. Y., Tronzo, C. R. *et al*. (1992) Relationships between cell volume and the carbon and nitrogen content of marine photosynthetic nanoplankton. *Limnol. Oceanogr.*, **37**, 1434-1446.

Wassmann, P., Ypma, J. E. and Tselepides, A. (2000) Vertical flux of faecal pellets and microplankton on the shelf of the oligotrophic Cretan Sea (NE Mediterranean Sea). *Prog. Oceanogr.*, **46**, 241-258.

Zervakis, V. and Georgopoulos, D. (2002) Hydrology and circulation in the North Aegean (eastern Mediterranean) throughout 1997 and 1998. *Mediterr. Mar. Sci.*, **3**, 5-19.

Zervakis, V., Ktistakis, M. and Georgopoulos, D. (2005) A new design for coastal drifters. *Sea Technology*, **46**, 25-30.

Zervoudaki, S., Christou, E. D., Nielsen, T. G. *et al*. (2007) The importance of small-size copepods in a frontal area of the Aegean Sea. *J. Plankton Res.*, **29**, 317-338.

Zhou, M. (2006) What determines the slope of a plankton biomass spectrum. *J. Plankton Res.*, **28**, 437-448.

TABLE AND FIGURE LEGENDS

Fig. 1. (a) Geographic location of the study area. The box identifies the region shown on a larger scale in (b) showing a synthetic diagram of the cruise. The tracks of the drifting sediment trap (deployed at 16 m depth), the control drifter and the ship have been overlaid on a map of surface salinity, obtained through the thermosalinograph. Numbers in circles indicate stations; (c) Time series of the longitude of: the sediment trap drifter (thick line), the ship (thin line) and the stations (open circles) performed during the experiment. Dark circles indicate additional CTD casts. Letters above the horizontal bar indicate the sediment trap deployment periods (duration in days is indicated in parentheses).

Fig. 2. Synoptic T-S diagram identifying the water types present (top) and temperature and salinity profiles (bottom) from CTD casts made at the stations along the drifter track. The large symbols in the T-S diagram represent the mean values in the 0 to 16 m layer.

Fig. 3. Comparison of water column production and composition to vertical flux (organisms and particles >5 μm) in the BSW layer (0-16 m integrated values). (a) POC concentration and C:N ratio of suspended POM; (b) unicellular plankton groups biomass; (c) zooplankton biomass; (d) net primary production >5 μm (percentages are ratios of net primary production >5 μm to total net primary production), mesozooplankton faecal pellet production; (e) POC flux and C:N ratio of sinking POM; (f) unicellular plankton C flux; (g) zooplankton carcasses C flux; (h) faecal C flux. See the correspondence between stations and trap deployment periods in Fig. 1c. f.p.: faecal pellet. AN: autotrophic nanoflagellates

Fig. 4. (a) Normalized biomass-size (NB-S) spectra (carbon) of the pico- to mesozooplankton community in all stations. Example of regression line plotted for Station 3 ($y = -1.10x+1.69$, $r^2 = 0.97$); (b) Temporal evolution of the BSW depth-integrated (0-16 m) community NB-S slopes. Standard error bars of the slopes are shown; (c) Relationship between NB-S slopes and total estimated carbon flux (from plankton cells, zooplankton carcasses and faecal pellets) ($r^2 = 0.95$; $P<0.01$).

Table I. Percentages of plankton components and detritus carbon (estimated) to total carbon (measured POC) in water column stations and sediment trap deployment periods. Sediment trap mesozooplankton (values with asterisks) include copepods <200 μm. UP: unicellular plankton; NM: not measured.

Table II. Elemental composition of sediment trap material collected during the 4 deployment periods. The values shown are averages (± sd) of pooled sediment trap samples (n = 4 for deployments A and B, and n = 3 for deployments C and D). Stable isotope values are in the per mil (‰) notation.

Plankton component or detritus	Station (water column) 2	3	5	6	8	Sediment trap deployment period A	B	C	D
Dinoflagellates	5.40	4.29	3.62	7.57	6.76	15.47	22.61	14.27	21.96
Other Flagellates	1.34	0.49	0.51	0.61	1.53	NM	NM	NM	NM
Diatoms	0.07	0.05	0.03	0.06	0.03	0.77	0.25	0.22	0.27
Coccolithophores	0.35	0.21	0.08	0.31	0.24	1.00	1.17	1.31	1.63
Ciliates	1.48	2.98	3.15	2.18	1.57	0.19	0.10	0.25	0.04
Total UP	8.64	8.02	7.38	10.72	10.12	17.44	24.13	16.04	23.91
Salps > 2mm	0.00	0.00	0.00	4.21	0.00	0.00	3.53	0.00	0.00
Chaetognaths > 2mm	3.28	0.31	1.72	3.21	3.74	0.00	3.53	0.00	0.00
Copepods >2mm	0.00	0.15	0.91	1.51	3.13	2.50	2.84	1.23	22.87
Mesozooplankton	4.34	4.99	9.72	6.99	13.42	8.48*	17.55*	25.08*	18.18*
Total Zoo	7.62	5.46	12.34	15.92	20.28	10.98	25.58	27.54	41.05
Total faecal pellets	NM	NM	NM	NM	NM	11.54	49.23	23.99	12.13

Deployment period	POC flux mg C m^{-2} d^{-1}	PON flux mg N m^{-2} d^{-1}	δ^{13}Corg (‰)	δ^{15}N (‰)	C:N
A	131 (22)	18 (5)	-24.0 (0.6)	4.6 (2.8)	8.6 (1.3)
B	189 (22)	29 (6)	-24.0 (1.0)	4.8 (1.9)	7.7 (0.7)
C	187 (44)	28 (13)	-24.3 (0.3)	2.4 (1.8)	7.8 (1.6)
D	311 (15)	47 (19)	-24.5 (0.3)	0.4 (3.4)	7.0 (1.2)

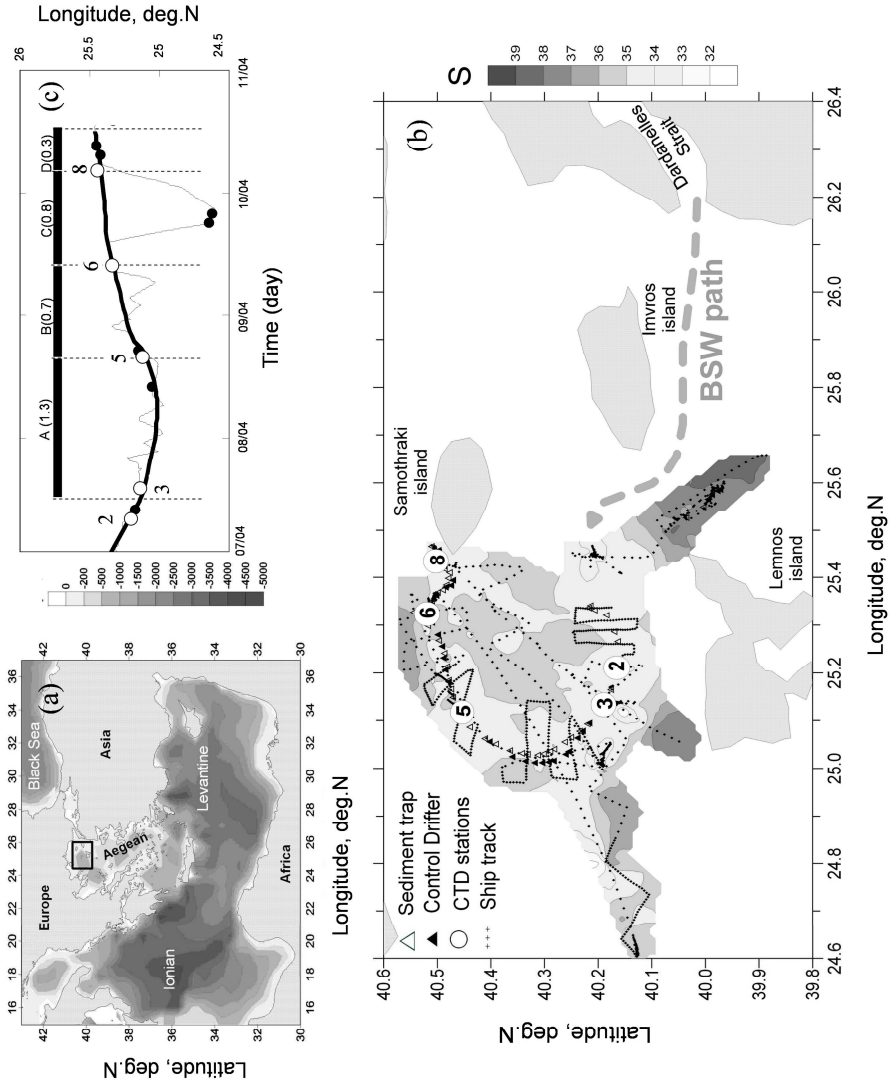

Fig. 1. (a) Geographic location of the study area. The box identifies the region shown on a larger scale in (b) showing a synthetic diagram of the cruise. The tracks of the drifting sediment trap (deployed at 16 m depth), the control drifter and the ship have been overlaid on a map of surface salinity, obtained through the thermosalinograph. Numbers in circles indicate stations; (c) Time series of the longitude of: the sediment trap drifter (thick line), the ship (thin line) and the stations (open circles) performed during the experiment. Dark circles indicate additional CTD casts. Letters above the horizontal bar indicate the sediment trap deployment periods (duration in days is indicated in parentheses).
374x426mm (300 x 300 DPI)

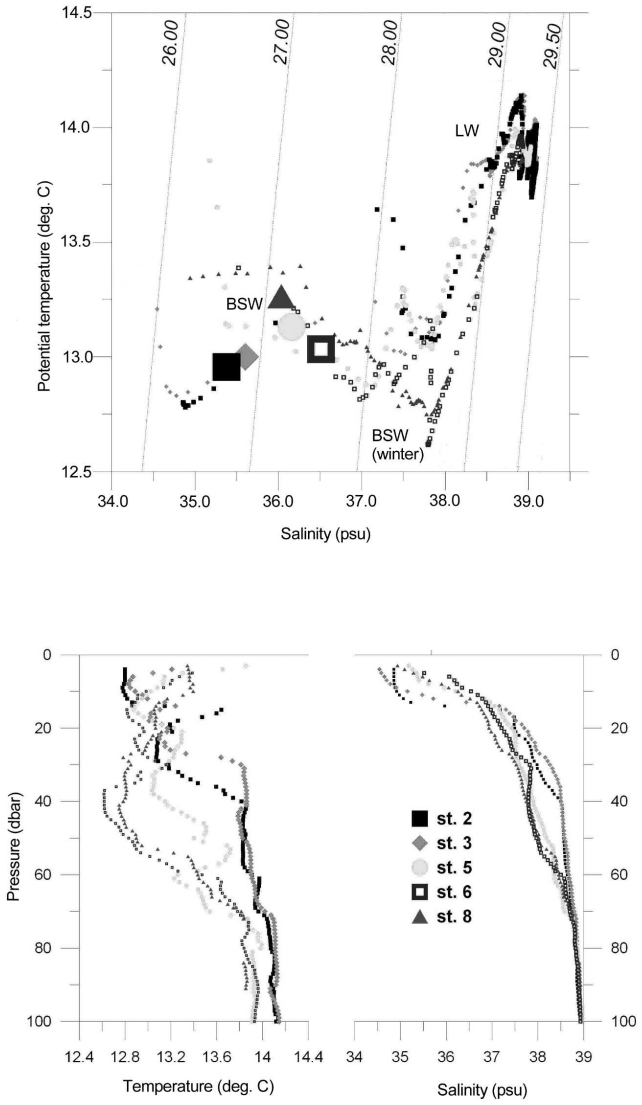

Fig. 2. Synoptic T-S diagram identifying the water types present (top) and temperature and salinity profiles (bottom) from CTD casts made at the stations along the drifter track (stations location indicated in Figure 1). The large symbols in the T-S diagram represent the mean values in the 0 to 16 m layer.
248x415mm (300 x 300 DPI)

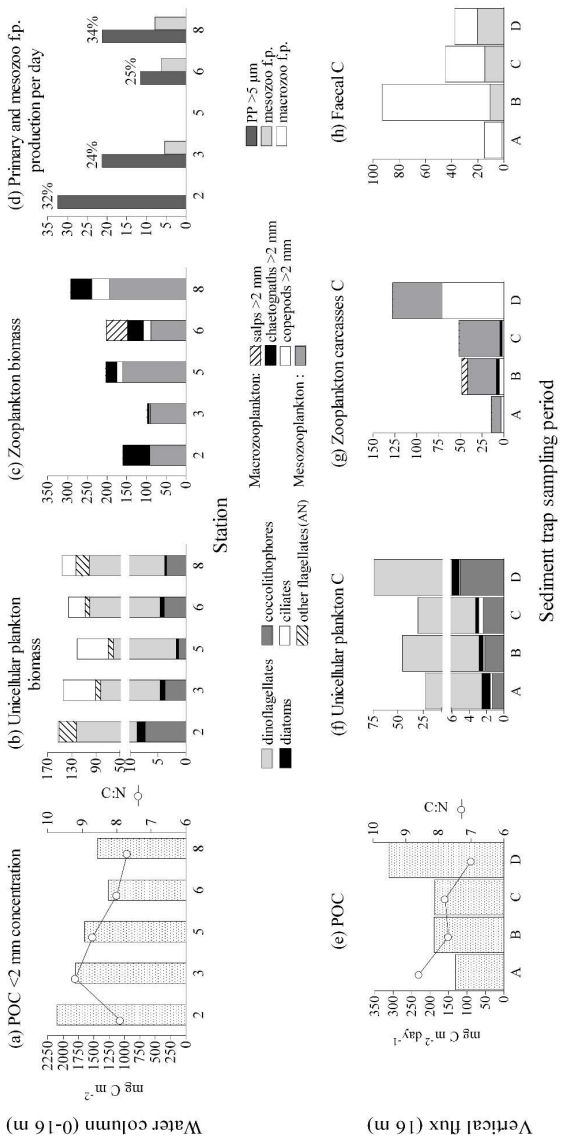

Fig. 3. Comparison of water column production and composition to vertical flux (organisms and particles >5 µm) in the BSW layer (0-16 m integrated values). (a) POC concentration and C:N ratio of suspended POM; (b) unicellular plankton groups biomass; (c) zooplankton biomass; (d) net primary production >5 µm (percentages are ratios of net primary production >5 µm to total net primary production), mesozooplankton faecal pellet production; (e) POC flux and C:N ratio of sinking POM; (f) unicellular plankton C flux; (g) zooplankton carcasses C flux; (h) faecal C flux. See the correspondence between stations and trap deployment periods in Fig. 1c. f.p.: faecal pellet. AN: autotrophic nanoflagellate
258x527mm (300 x 300 DPI)

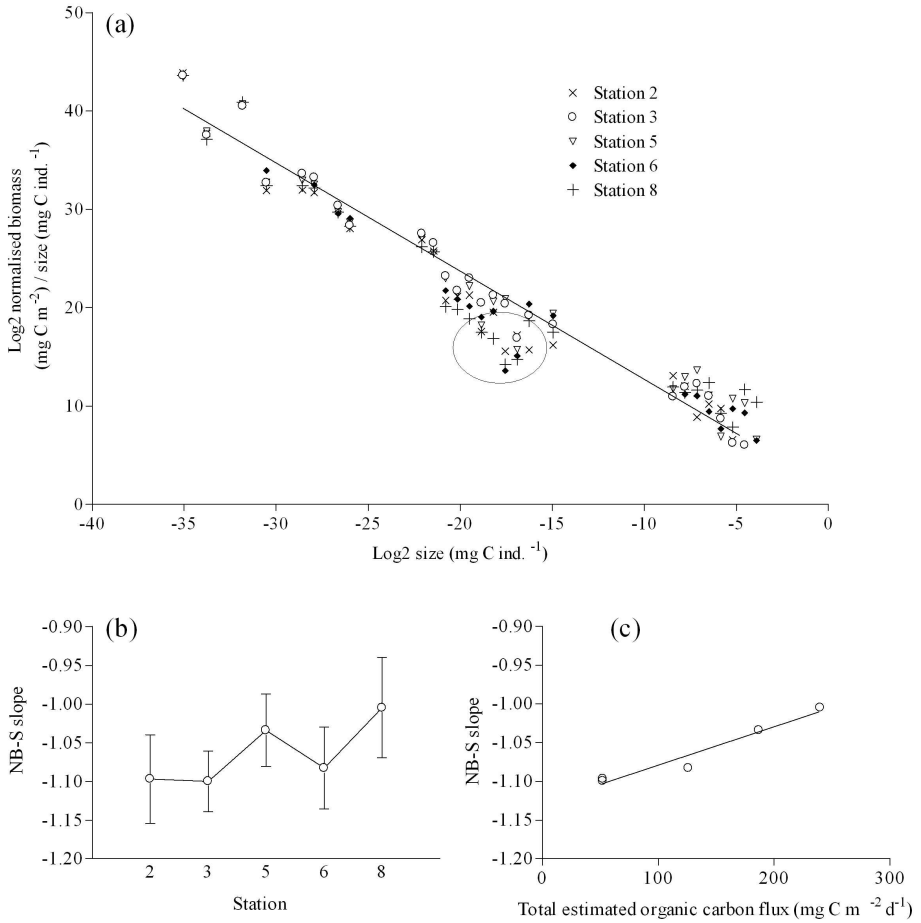

Fig. 4. (a) Normalized biomass-size (NB-S) spectra (carbon) of the pico- to mesozooplankton community in all stations. Example of regression line plotted for Station 3 (y = -1.10x+1.69, r2 = 0.97); (b) Temporal evolution of the BSW depth-integrated (0-16 m) community NB-S slopes. Standard error bars of the slopes are shown; (c) Relationship between NB-S slopes and total estimated carbon flux (from plankton cells, zooplankton carcasses and faecal pellets) (r2 = 0.95; P<0.01).
215x247mm (300 x 300 DPI)